JPPIPA 11(6) (2025)

Jurnal Penelitian Pendidikan IPA

http://jppipa.unram.ac.id/index.php/jppipa/index

Compacted Dry Biocellulose Formulated from Xanthosoma Undipes K. Koch (Taro): Characterization of Physical and Chemical Properties

Septia Ardiani[1*], Handika Dany Rahmayanti[2], Nurul Akmalia[3], Annisa Jasmine[2]

[1] Machine Maintenance Study Program, Industrial Technology,Politeknik Negeri Media Kreatif, Jakarta, Indonesia.
[2] Packaging Engineering Technology, Industrial Technology,Politeknik Negeri Media Kreatif, Jakarta, Indonesia.
[3] Photography, Communication, Politeknik Negeri Media Kreatif, Jakarta, Indonesia.

Received: April 19, 2025
Revised: May 20, 2025
Accepted: June 25, 2025
Published: June 30, 2025

Corresponding Author:
Septia Ardiani
septiaardiani@polimedia.ac.id

DOI: 10.29303/jppipa.v11i6.11098

Abstract: This study aims to evaluate the physical properties of compacted dry biocellulose derived from Xanthosoma undipes K. Koch (taro). Three types of substrates were fermented using Acetobacter xylinum: nata de taro (NDT), nata de coco-taro (NDC-T), and nata de coco-taro-pineapple-tomato (NDC-TPT). The resulting biocellulose products were compacted using a hot press (5000 kgf/cm² for approximately 15 minutes at 120°C) and then dried at 30°C to produce solid biopolymer sheets. Characterization included thickness measurement, FTIR spectroscopy, UV-Vis spectroscopy, and SEM-EDX microscopy. Results showed that the cellulose chemical structure remained intact after compaction. The NDC-TPT sample exhibited the highest porosity and water absorption capacity, along with significant UV light transmittance, making it a promising candidate for biodegradable film applications and active moisture-absorbing materials. Microscopic analysis revealed that substrate composition strongly influenced fiber density and pore size, with NDT showing the densest structure and NDC-TPT the most porous.

Keywords: FTIR; SEM; Thickness; UV-Vis

Introduction

Biocellulose from dried and compacted nata de coco (NDC) is a material that is capable of absorbing water vapor comparable to the absorption capacity of silica gel or higher (Rahmayanti et al., 2024). In the water absorptivity test, several commercial NDCs and silica gels available in the market were tested on sponge cake products. Three brands of NDC showed higher absorption than silica gel and this value continued to increase from day 1 to day 5. The amount of water absorbed by the NDC sample on day 5 was 15.087% (brand B); 21.86% (brand C) and 22.664% (brand F). This value is greater when compared to the absorption by silica gel on sponge cake, which is 15.532% (Rahmayanti et al., 2022). In addition, dry and compressed NDC is also able to extend the shelf life of apples, mangoes and pears (Rahmayanti et al., 2019).

Dry compacted nata de coco (NDC) has been shown to be a promising alternative to silica gel for absorbing water vapor in food products, thereby extending shelf life. This material has already been utilized in various commercial products marketed by MSMEs under the Saung Taleus Group, including taro flour, ketapang seeds, cakes, and pies (Rahmayanti, 2021). However, large-scale production of compacted dry NDC is constrained by the declining availability of coconut water, its primary raw material. This is due to the annual decrease in coconut production in Indonesia—estimated at -1.086%—caused by land degradation, aging

How to Cite:
Ardiani, S., Rahmayanti, H. D., Akmalia, N., & Jasmine, A. (2025). Compacted Dry Biocellulose Formulated from Xanthosoma Undipes K. Koch (Taro): Characterization of Physical and Chemical Properties. *Jurnal Penelitian Pendidikan IPA*, *11*(6), 487–497. https://doi.org/10.29303/jppipa.v11i6.11098

plantations, and farmers shifting to other crops (Afdal S et al., 2019). Additionally, increasing exports of whole coconuts have reduced domestic availability for processing, with Indonesia's copra exports expected to fall to 2,246,601 tonnes in 2025 (Darmawan et al., 2023). In this context, utilizing taro as an alternative substrate offers a strategic and sustainable solution to ensure continued NDC production, given its high carbohydrate content suitable for nata fermentation.

Figure 1. Use of dry compacted NDC in food products by MSMEs under the Saung Taleus Group

The process of making this material involves pressing NDC using a hot press at a temperature that allows water to escape without damaging the physical properties of the material, resulting in dry biocellulose with a very low water content. This material is cut into square shapes measuring 1 cm × 1 cm as seen in figure 2 (Ardiani et al., 2023; Rahmayanti et al., 2019). Then it is wrapped in strong reticulated paper consisting of a waterproof layer, fiber layer and polyethylene layer so that it is safe to use (Amarakoon et al., 2017). Measurements were made by directly weighing the mass of all NDCs.

However, mass production of NDC faces challenges due to the decreasing supply of coconut water as the main raw material. Indonesian coconut production has experienced an annual decline of -1,086% due to land shrinkage, crop damage, and commodity switching by farmers (Afdal S et al., 2019). The increase in whole coconut exports also narrows the supply for domestic needs, including the manufacture of NDCs (Darmawan et al., 2023). Therefore, exploration of alternative raw materials such as taro is a strategic step to overcome this limitation.

Biocellulose has traditionally been produced from coconut water due to its abundance and fermentable sugar content. However, recent studies have highlighted the potential of *Xanthosoma undipes* K. Koch (taro), a tropical plant rich in starch and fiber, as an alternative source of biocellulose. Taro contains high levels of complex carbohydrates—primarily starch and sugars—which can be utilized by *Acetobacter xylinum* during fermentation to synthesize nata (Maulani et al., 2018). In particular, wastewater from starch extraction of Beneng taro has been demonstrated to support nata production when supplemented with sucrose, acetic acid, and nitrogen sources. A study by Maulani et al. (2018) found that the use of 25% inoculum yielded nata with a thickness of 9.55 mm and crude fiber content of 4.89%. Although such studies confirm the viability of taro-based substrates for nata production, the development and characterization of *compressed dry biocellulose* from taro remain largely unexplored.

Figure 2. NDC dry compacted size 1 cm x 1 cm

One potential candidate is Xanthosoma undipes K. Koch (taro), a tropical plant rich in fiber and cellulose. Taro has a high content of complex carbohydrates—starch and sugar—which allows fermentation by Acetobacter xylinum to produce nata (Maulani, 2018). This plant grows widely in Indonesia and is starting to be widely cultivated in Banten and West Java making it a sustainable source of raw materials (Suhaendah et al., 2021).

This study also varied the substrate with the addition of pineapple (Ananas comosus) and tomato (Solanum lycopersicum), the production of which in Indonesia continues to increase and is known to be able to produce good quality nata (Krissanjaya, 2024). Substrate variation aims to improve the physical and chemical characteristics of the resulting biocellulose, such as thickness, porosity, and water absorption.

The novelty of this study lies in the formulation and characterization of compressed dry biocellulose made from taro-based substrates, with a focus on comparing the physical and chemical properties of biocellulose derived from single and mixed substrates. Understanding how substrate composition affects material performance is critical for the development of

next-generation biodegradable films and active moisture absorbing materials. As the demand for sustainable and environmentally friendly packaging and storage materials increases, this research provides important insights to optimize biocellulose properties for wider commercial and industrial applications.

To date, research on the physical and chemical characteristics of compressed dry NDC has indeed been quite developed (Rahmayanti et al., 2019, 2022), and several studies have discussed nata production from various raw materials. However, there has been no research that systematically compares the physical and chemical properties of biocellulose based on single substrates (nata de taro) and mixed substrates (nata de coco-taro and nata de coco-taro-pineapple-tomato) in dry compressed form. This research gap is important to fill in order to broaden the understanding of the impact of substrate formulation on the performance of the final material, especially in relation to moisture absorber applications and environmentally friendly packaging.

To support this objective, thickness tests were carried out to evaluate the homogeneity and stability of the material shape; FTIR to identify chemical functional groups (Fuller et al., 2018); UV-Vis to assess the optical properties of the material relevant in transparent film applications (Guzman-Puyol et al., 2022) and SEM-EDX to observe surface morphology and elemental composition (Adhikari et al., 2023). This approach provides an in-depth understanding of how substrate composition affects the final material properties, which has not been widely discussed in previous studies. With this comprehensive characterization, it is hoped that the suitability of compressed dry biocellulose from taro can be assessed as a base material for environmentally friendly packaging applications or as an alternative to silica gel.

Method

Substrate making is the initial stage in this research. There are three types of biocellulose made, namely nata de taro (NDT), nata de coco-taro (NDC-T), and nata de coco-taro-pina-tomato (NDC-TPT). The substrates needed to make this biocellulose are taro, coconut water, pineapple, and tomato. 1) For NDT, taro substrate is obtained by sorting 1 kg of taro of the Xanthosoma undipes K. Koch type, removing dirt and washing it clean. The clean taro is cut into cubes, mashed with a blender. The smooth taro is added with 1 L of water and precipitated for 24 hours until the water and starch are separated. The water from the starch sediment is the taro substrate that will be used as raw material for making nata de taro (Maulani et al., 2018). 2) For NDC-T, taro substrate is mixed with coconut water in a ratio of 1:1. 3) And for NDC-TPT, taro substrate is obtained by method 1. Tomato substrate and pineapple substrate are obtained by preparing raw materials of pineapple type Ananas comosus (L.) Merr and tomato type Solanum lycopersicum. The raw materials are washed and cut into small pieces. Furthermore, the raw materials are blended to make them smooth. Filtering using calico to separate the filtrates and the residues (Sutanto, 2012). Taro substrate, coconut water, pineapple substrate, and tomato substrate are mixed in a ratio of 3:3:2:2.

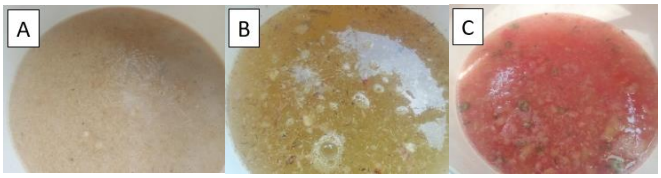

Figure 3. Substrate (a) taro, (b) pineapple, and (c) tomato

Table 1. Biocellulose Material Composition

Items	NDT	NDC-T	NDC-TPT
Substrate	100% taro	50% taro, 50% coconut water	30% taro, 30% coconut water, 20% pineapple, 20% tomato
Ph	3	3	3
Sugar content	3,5% Brix	4% Brix	7% Brix
Starter	150 mL	150 mL	150 mL

The main ingredients for making NDT, NDC-T and NDC-TPT biocellulose are taro substrate, coconut water, pineapple substrate, tomato substrate, sucrose, ammonium sulfate, Acetobacter Xylinum seeds, and other additives. The following is the composition of making biocellulose.

The next process is carried out by following the NDT manufacturing technique (Gayathry, 2015). The main ingredients are weighed using an analytical balance and a measuring cup. The substrate as much as 5 liters is boiled and added with 250 g of sucrose, 70 g of ammonium sulfate, and 100 mL of acetic acid. The media is cooled to a temperature of 25^{o}C and the acidity level is measured using a pH meter. Then add the nata starter Acetobacter xylinum. The container is covered with paper so as not to be contaminated by other bacteria and fermented for 9 days on the fermentation rack. The best fermentation for nata de taro is 9 days (Salelatu et al., 2016), pineapple nata 8-14 days (Novia et al., 2021), and nata de tomato 9-14 days (Mustain et al., 2022). The

biocellulose is then ready to be harvested and analyzed (Maulani et al., 2018). The harvested biocellulose can be seen in Figure 4.

Figure 4. (a) NDT, (b) NDC-T, and (c) NDC-TPT

After nata is harvested, the weight and thickness of biocellulose are measured. Measurements are made to ensure that the biocellulose used has the same characteristics. Cellulose weight is measured using an analytical balance and thickness using a vernier caliper. Weighing is done after the nata is drained for ±10 minutes (Rahmayanti et al., 2024). For samples with characteristics that are not the same, equalization is carried out.

Table 2. Biocellulose Measurement Results Data

Items	NDT	NDC-T	NDC-TPT
Total media (mL)	1090±40	1037±26	1783±59
Cellulose mass (g)	240±21	441±29	800±36
Vol. of residual (mL)	700±20	447±21	834±31
Yield (%)	22±2	43±4	45±1
Thickness (cm)	0.87±0.13	1.19±0.13	1.62±0.14

The uniformity of thickness and mass of biocellulose in each sample is the most important quantity in characterizing the physical and mechanical properties of compacted dry biocellulose. Biocellulose was sliced using a slicer machine to obtain uniform thickness and mass.

The main materials used for the formulation of compacted dry biocellulose are NDT, NDC-T, and NDC-TPT, which were obtained from the previous fermentation process. Additional components include 98% acetic acid, 70% ethanol, chitosan, glycerol, and other additives. The primary equipment used in the natagel production process is a hot press. Initially, the biocellulose is soaked to remove residual sugar content. Subsequently, the water-laden biocellulose is compacted using a hot press at a pressure of 5000 kgf/cm² for approximately 15 minutes at 80°C. After pressing, the biocellulose sheets are sun-dried for 5 hours at an ambient temperature of 30°C to produce solid biopolymer films. The resulting pressed and dried biocellulose is then subjected to physical and morphological characterization as a preliminary assessment to compare its properties with those of NDC.

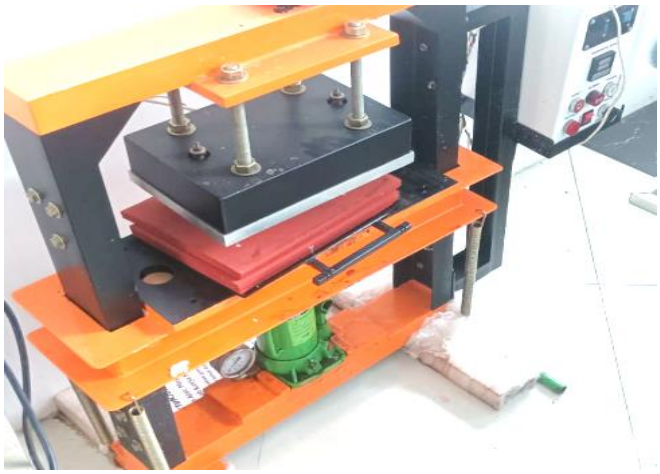

Figure 5. Hot press machine

Several characterizations have been employed such as physical properties and morphological properties as well as unit structures. To examine the sample transmittance an UV-VIS spectrometer was applied (Rahmayanti et al., 2018). From the FTIR test, it was observed that the functional groups formed from compacting dry bioselulose from NDT, NDC-T, and NDC-TPT (Latif et al., 2023). Morphology testing of compacted dry biocellulose was carried out using SEM-EDX as can be seen in Figure 6.

Figure 6. SEM-EDX test on compacted dry biocellulose

Result and Discussion

The biocellulose produced has three models, namely NDT, NDC-T, and NDC-TPT. These three biocellulose models are the main raw materials for making compacted dry biocellulose. This raw material has a very varied thickness and mass. The thickness variation ranges from 0.74 cm to 1.76 cm while the biocellulose mass variation is 219 g to 836 g (see table 2). For testing the physical properties of compacted dry biocellulose, the main raw material must have the same thickness so that the results of the compacted dry

biocellulose test are more accurate and representative (Yano et al., 2007). Uniform raw material thickness will minimize variations in the results of measuring the physical properties of compacted dry biocellulose such as the UV-Vis test (Clasen et al., 2006), thickness (Nur et al., 2023), and FTIR test (Agarwal et al., 2017). Uniforming the thickness of the raw material using a slicer machine is 0.8 cm referring to the lowest thickness of biocellulose produced (NDT). Apart from the thickness of the raw material, the mass of the raw material also determines the accuracy of the results of characterization of the physical properties of compressed dry biocellulose (Yasa et al., 2020). Below is data on the mass of biocellulose at a thickness of 0.8 cm. From the table it can be seen that uniforming the thickness of the raw material also uniformizes the mass. The thickness of the raw material is proportional to the mass (Hamad et al., 2016).

Table 3. Mass of Biocellulose at a Thickness of 0.8 cm

Items	Massa (g)		
	Sample 1	Sample 2	Sample 3
NDT	244	260	249
NDC-T	257	240	265
NDC-TPT	233	242	240
Average	245	247	251
Standard Deviation	12	11	13

Biocellulose was processed using a hot press machine with a pressure of 5000 kgf/cm^2 for ±15 minutes (Rahmayanti et al., 2022) at a temperature of 120^{o}C (Rahmayanti et al., 2019) and dried at room temperature. The results of this compacted dry biocellulose can be seen in Figure 7. The temperature and pressure are the optimum values obtained from several experiments that have been carried out to produce a thin layer without damaging the structure of the NDC (Rahmayanti et al., 2024). The three samples of compacted dry biocellulose produced were named sample A (NDT bisocellulose raw material), sample B (NDC-T bisocellulose raw material), and sample C (NDC-TPT bisocellulose raw material).

Figure 7. (a) Dry compacted NDT (sample A), (b) Dry compacted NDC-T (sample B), and (c) Dry compacted NDC-TPT (sample C)

After densification and drying at room temperature, the final thickness of each sample was measured. The thickness of the compacted dry Biocellulose was measured using a vernier caliper using a 10 cm x 10 cm sample. Then determine 10 points randomly in the area. As shown in Table 4, the NDC-TPT sample yielded the greatest average thickness, whereas NDC-T had the lowest. But overall, all three have almost the same thickness. Because the thickness and mass of the raw materials are the same (Yasa et al., 2020).

Table 4. The Thickness of the Dry Compacted Cellulose

Items	Average thickness (cm)
NDT dry compacted	0.054 ± 0.011
NDC-T dry compacted	0.047 ± 0.018
NDC-TPT dry compacted	0.063 ± 0.006

Fourier Transform Infrared (FTIR) spectroscopy was used to identify the functional groups present in the dried-densified bioselulosa. The FTIR spectrum for sample A is shown in Figure 8. The spectrum indicates the presence of several characteristic absorption bands corresponding to cellulose. The broad absorption band around 3300–3400 cm^{-1} indicates O–H stretching vibration of hydroxyl groups, a key feature in the cellulose structure. The peaks observed near 2900 cm^{-1} are attributed to C–H stretching of aliphatic –CH groups. The peak at 1630–1650 cm^{-1} indicates the presence of adsorbed water, which is common in hydrophilic materials such as bacterial cellulose. This is lower compared to the dried-densified NDC (Syaifudin et al., 2015)(Rahmayanti et al., 2019; Syaifudin et al., 2015). The region around 1430 cm^{-1} reflects CH_2 bending, and around 1370 cm^{-1} is associated with C–H deformation. The peak at 1050–1100 cm^{-1} is a strong signal of C–O–C stretching, confirming the presence of β-glycosidic linkages between glucose units in cellulose. These findings confirm that the chemical structure of cellulose remains intact during the densification process, with no significant degradation of key functional groups.

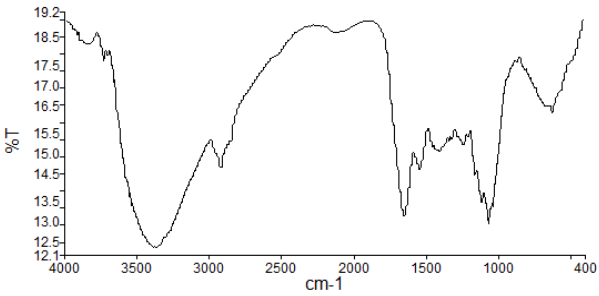

Figure 8. FTIR spectrum of NDT (Sample A)

The FTIR analysis of Sample B (Figure 9) confirms the preservation of functional groups associated with bacterial cellulose. A broad O–H stretching vibration is

observed around 3300–3400 cm^{-1}, indicating the presence of hydroxyl groups. Peaks at 2900 cm^{-1} and 1430 cm^{-1} correspond to C–H stretching and CH_2 bending vibrations, respectively. A distinct peak at 1650 cm^{-1} is attributed to adsorbed water molecules. Similar to Sample A, the water absorption peak is lower compared to pure dried-densified NDC (Rahmayanti et al., 2019). The prominent peak around 1050–1100 cm^{-1} confirms the presence of β-1,4-glycosidic linkages, which are characteristic of cellulose. These results indicate that the densification process preserves the structural integrity of the bioselulosa material.

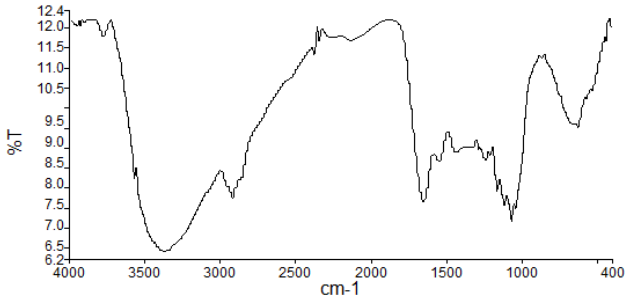

Figure 9. FTIR spectrum of NDC-T (Sample B)

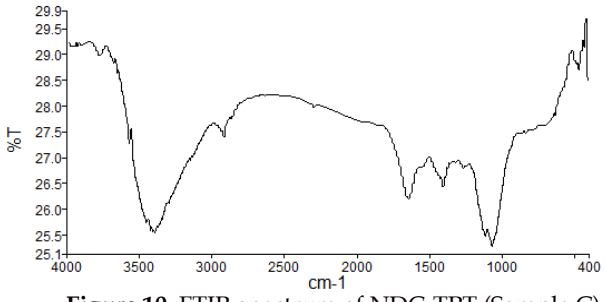

Figure 10. FTIR spectrum of NDC-TPT (Sample C)

The spectrum of Sample C reveals the characteristic functional groups associated with cellulose and polysaccharide structures. The FTIR graph is presented in Figure 10. A broad and intense absorption band is observed around 3330–3360 cm^{-1}, corresponding to the O–H stretching vibrations of hydroxyl groups. This broad peak suggests the presence of extensive hydrogen bonding, which may result from the synergistic contribution of multiple cellulose-rich and pectin-containing raw materials, such as pineapple and tomato (Hamad et al., 2016). The C–H stretching vibration appears at approximately 2900 cm^{-1}, indicating the aliphatic –CH_2 groups commonly found in the cellulose backbone. The region around 1650 cm^{-1} corresponds to the H–O–H bending vibrations of adsorbed water, which is typical for hydrophilic materials like bioselulosa. Bands at 1425 cm^{-1} and 1370 cm^{-1} are assigned to the CH_2 scissoring and C–H bending modes, respectively. A strong and sharp absorption band at 1050–1100 cm^{-1} is attributed to C–O–C stretching vibrations of the β-1,4-glycosidic linkages, which are definitive indicators of cellulose structure. Furthermore, weak absorption below 900 cm^{-1} falls within the cellulose fingerprint region, reinforcing the cellulose identity of the bioselulosa matrix. Interestingly, the transmittance values of Sample C were significantly higher (25–30% T) compared to Samples A and B, suggesting a potential decrease in crystallinity or a more amorphous structure of the cellulose matrix due to the incorporation of diverse fruit-derived biomasses. This amorphous behavior may enhance certain physical properties, such as flexibility or permeability, which are beneficial for applications in biodegradable film or packaging materials (Cheng et al., 2024; Shaikh et al., 2021).

Table 5. Comparative Analysis of the FTIR of Dry Compacted Biocellulose

FTIR Feature	Sample A	Sample B	Sample C
O–H Stretch (~3300 cm^{-1})	Broad, strong	Slightly less intense	Broadest, suggesting higher H-bonding
C–H Stretch (~2900 cm^{-1})	Present	Present	Present
H–O–H Bend (~1650 cm^{-1})	Moderate	Similar	Similar
C–O–C Stretch (~1050–1100 cm^{-1})	Distinct, sharp	Slightly broader	Strong and prominent
Transmittance Intensity (%T)	~12–19%	~6–12%	~25–30% (much higher)

Table 5 highlights the differences among the three types of samples. Derived solely from taro, the FTIR spectrum of Sample A is clean and rich in cellulose. The prominent O–H and C–O–C peaks reflect pure bioselulosa with minimal interference from other plant materials. For Sample B, the combination of coconut and taro results in a denser hydrogen bonding network, though the spectrum appears slightly broader. The lower transmittance values suggest tighter molecular packing or a higher cellulose content per volume. In the case of Sample C, the inclusion of pineapple and tomato alongside coconut and taro appears to introduce additional bioactive components or polysaccharides. The overall higher transmittance may indicate a more porous structure or lower crystallinity. This porosity enables the dried-densified bioselulosa to absorb water most effectively. The broader O–H stretching suggests more hydrogen-bonded hydroxyl groups, potentially from cell wall polysaccharides in tomato and pineapple, such as pectin or hemicellulose.

The UV-Vis absorbance spectrum of the dry compacted bioselulosa synthesized from nata de taro

(Sample A) is shown in Figure 11. The scan was conducted in the range of 200–1200 nm, with three significant peaks observed at approximately ~260 nm (Peak 3), ~370 nm (Peak 2), and ~800 nm (Peak 1). The absorbance maximum around 260 nm corresponds to π → π* transitions typical of C=C bonds, which may indicate residual organic compounds or minor lignin-like structures present due to the taro substrate. This is commonly associated with aromatic or conjugated systems in plant-based cellulose precursors (Clasen et al., 2006). The second peak at around 370 nm suggests the presence of n → π* transitions related to carbonyl (C=O) groups, possibly from oxidized saccharides or minor impurities in the substrate. It indicates some degree of chemical modification or bonding interactions within the cellulose matrix. The third peak around 800 nm is less commonly observed in pure cellulose and may be an artifact or related to scattering or residual impurities, though its sharp spike and irregularity suggest the limitations of the detection system at the longer wavelength range. Overall, the UV-Vis spectrum indicates that Sample A possesses optical absorbance properties dominated in the UV range (200–400 nm), suggesting a relatively clean cellulose matrix with minimal chromophoric impurities and moderate UV-blocking capability. This implies potential applicability in UV-shielding films or packaging materials.

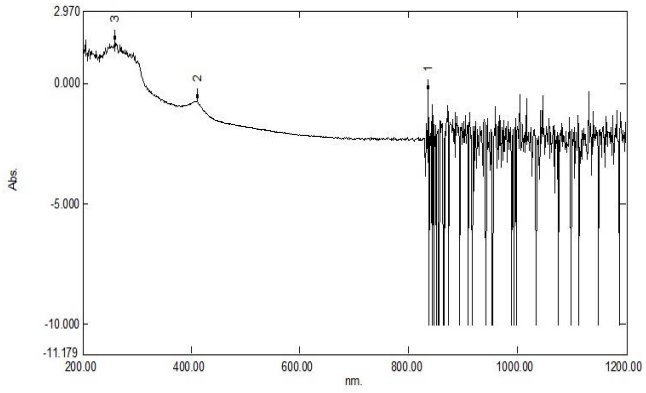

Figure 11. UV-Vis sample A

Sample A exhibited a prominent absorbance peak at approximately 280–290 nm, with a maximum absorbance value of around 2.97. This strong peak is indicative of the presence of aromatic compounds, such as phenolics or amino acid derivatives typically found in taro. A smaller shoulder was observed near 370 nm, suggesting the presence of minor conjugated compounds. The absorbance remained relatively flat in the visible region (400–700 nm), indicating the absence of significant pigments.

Sample B showed a similar absorbance profile, with a major peak around 280–290 nm and a lower maximum absorbance of approximately 2.39. This reduction in intensity may be attributed to the dilution or interaction of taro compounds with coconut constituents, which contribute less to UV-absorbing species. As in Sample A, the visible and near-infrared regions did not show notable features aside from noise beyond 800 nm.

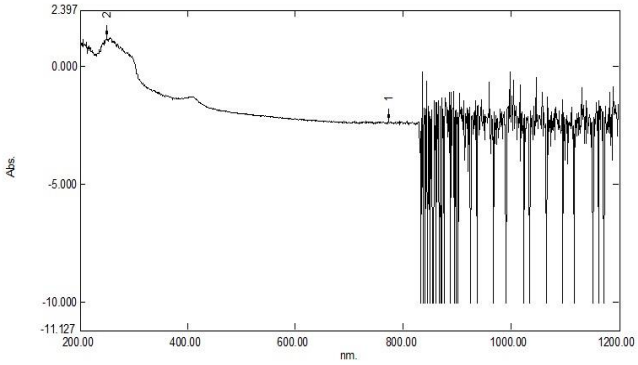

Figure 12. UV-Vis sample B

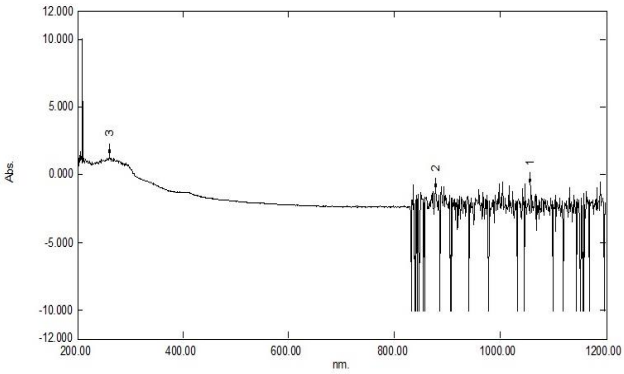

Figure 13. UV-Vis sample C

In contrast, Sample C demonstrated a substantially higher absorbance at the 280–290 nm region, reaching a maximum of ~6.00, indicating a significantly increased concentration of UV-absorbing compounds. This enhancement is likely due to the inclusion of pineapple and tomato, both of which are rich in vitamin C, carotenoids, and flavonoids. Although no distinct peaks were observed in the visible range, a slight elevation in the baseline suggests the presence of broad-spectrum pigments, possibly from lycopene and β-carotene. The near-infrared region again showed noise and was not considered for analysis.

The UV-Vis absorbance spectra of Sample A (nata de taro), Sample B (nata de coco–taro), and Sample C (nata de coco–taro–pina–tomato) were analyzed within the wavelength range of 200–1200 nm to evaluate the presence of water-interacting compounds and their potential application in food products, particularly as water-absorbing or moisture-retaining ingredients.

Table 6. Comparative Analysis of the UV-Vis

Features	Sample A	Sample B	Sample C
Max absorbance (280–290 nm)	~2.97	~2.39	~6.0
Presence of visible-range activity	Low	Very low	Slight slope (broad absorption)
Likely bioactive compounds	Phenolics, amino acids	Fewer phenolics	Phenolics, carotenoids, flavonoids
IR noise	Present	Present	Present

Sample A showed a strong absorbance peak at approximately 280–290 nm, with a maximum absorbance of ~2.97. This suggests a high presence of hydrophilic compounds, such as phenolic substances and amino acid derivatives, which are known to contribute to water-binding capacity. The composition of taro-based nata likely includes polysaccharides or starch-like molecules, enhancing its ability to absorb and retain water in food formulations. Sample B, which includes both coconut and taro, exhibited a similar peak around 280–290 nm, but with a slightly lower intensity (~2.39). This may be due to the reduced concentration of UV-absorbing compounds, as coconut generally contributes more lipophilic than hydrophilic components. Nevertheless, the presence of taro still supports moderate water absorption, making this sample suitable for texture enhancement and moisture retention in semi-moist food products. Sample C displayed the most intense absorbance at the 280–290 nm region, reaching a maximum of ~6.00. This indicates a significantly higher concentration of bioactive and water-attracting compounds, likely due to the inclusion of pineapple and tomato, which are rich in organic acids, vitamin C, flavonoids, and natural sugars. These compounds enhance the sample's hydrophilic nature, suggesting that Sample C possesses superior water absorption capacity, which could be beneficial for applications such as hydrated gels, edible films, or high-moisture functional foods. In all samples, the noisy signals beyond 800 nm were disregarded as instrumental artifacts. No strong absorption was observed in the visible region (400–700 nm), though Sample C showed a slight baseline elevation, possibly indicating the presence of light-absorbing pigments with water-soluble properties.

The surface morphology of the biosynthesized dry compacted bioselulosa from different substrate combinations was analyzed using Scanning Electron Microscopy (SEM) at 7500× magnification (Figure 14).

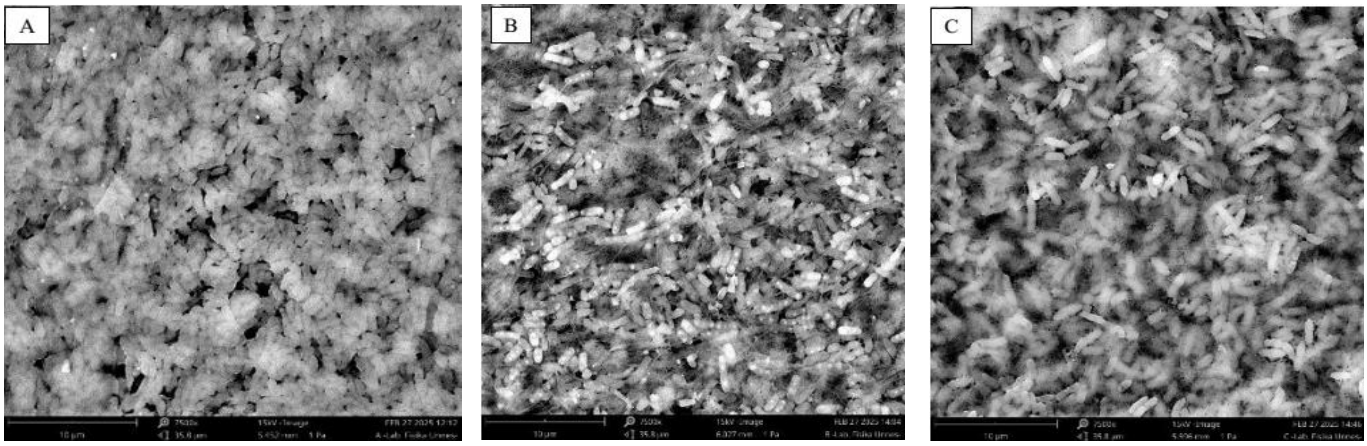

Figure 14. Morphology with 7500x magnification (a) dry compacted NDT, (b) dry compacted NDC-T, and (c) dry compacted NDC-TPT

Each sample showed distinct microstructural characteristics influenced by its fermentation media composition. Sample A (NDT) exhibited a dense and compact cellulose network with tightly packed nanofibers arranged in a uniform and orderly fashion. The fibrils were relatively fine and interconnected, forming a coherent three-dimensional structure. This morphology is indicative of high crystallinity and structural integrity, which is typical of bacterial cellulose synthesized from a single, consistent carbohydrate source like taro. The smooth and continuous surface suggests minimal impurities, leading to potentially better mechanical strength and thermal stability (Yano et al., 2007). Sample B (NDC-T) presented a less compact fiber arrangement compared to Sample A. The presence of coco substrate altered the fiber formation, leading to slightly larger pores and a looser fibril network. While still maintaining a relatively ordered structure, the addition of coconut water seemed to promote a more porous and less uniform microstructure. This can be attributed to the natural sugars and minerals present in coconut, which may interfere with the bacterial cellulose

biosynthesis and affect the rate and orientation of fibril deposition (Nur et al., 2023). Sample C (NDC-TPT) demonstrated the most disordered and porous morphology among all three samples. The SEM image revealed larger voids, irregular fibril distribution, and a more fragmented network. The incorporation of pineapple and tomato, in addition to taro and coconut, appears to have significantly influenced the bacterial activity and cellulose structuring. The irregularities and nodular textures observed suggest the presence of residual non-cellulosic materials or enzymatic activity that disrupted the typical nanofiber formation (Rahmayanti et al., 2024). Although structurally weaker, this morphology could provide advantages in applications requiring high water absorption, flexibility, or functionalization.

Table 7. Comparative Analysis of the Morphology

Item	Morphology Characteristics	Fiber Density	Pore Size	Surface Uniformity
NDT	Dense, uniform nanofibers	High	Small	Smooth
NDC-T	Moderately compact, slightly porous	Moderate	Medium	Slightly irregular
NDC-TPT	Loose, porous, and irregular	Low	Large	Rough, nodular

Morphological analysis of the three types of samples—NDT (derived from taro), NDC-T (a combination of taro and coconut), and NDC-TPT (a combination of taro, coconut, tomato, and pineapple)—revealed significant differences in physical structure that directly affect water absorption capacity (Table 7). The NDT sample exhibited a dense and uniform nanofiber morphology with high fiber density and small pore size. Its smooth surface indicates minimal space for water penetration, suggesting that this structure is more suitable for applications requiring a moisture barrier rather than absorption. This is consistent with the characteristics of pure cellulose, which typically has high crystallinity and low porosity. In contrast to NDT, the NDC-T sample showed a more open structure, with moderate fiber density and medium pore size. The slightly irregular surface indicates increased material heterogeneity due to the addition of coconut. This structure allows for a moderate increase in water absorption capacity, although it is not as efficient as a highly porous structure. Meanwhile, the NDC-TPT sample exhibited the loosest and most irregular morphology, with low fiber density and large pore size. The rough and nodular surface suggests a significant increase in active surface area, supporting higher water absorption. The addition of bioactive components from tomato and pineapple contributes to the formation of this structure and enriches the sample with hydrophilic polysaccharides such as pectin and hemicellulose. These characteristics allow NDC-TPT to absorb moisture most effectively among the three samples, making it the best candidate for active packaging applications or as a moisture-absorbing material in food preservation systems. Thus, it can be concluded that morphological differences induced by variations in raw materials directly influence water absorption capacity, with more porous, irregular, and loose structures delivering superior moisture absorption performance.

Conclusion

This study demonstrates that compacted dry biocellulose derived from taro (NDT), coconut–taro (NDC-T), and coconut–taro–pineapple–tomato (NDC-TPT) substrates can serve as viable alternatives to conventional moisture-absorbing materials like silica gel. All three samples retained the fundamental cellulose structure after the densification process, with compositional differences significantly affecting their physical, chemical, and morphological properties. NDC-TPT, in particular, exhibited the highest porosity, UV transmittance, and water absorption, making it especially promising for applications in biodegradable films, functional food packaging, and active humidity control materials. These findings suggest that the formulation of fermentation substrates can be strategically adjusted to optimize biocellulose properties for various industrial applications. The results also offer broader implications for the use of underutilized agricultural resources, like taro, in developing sustainable packaging materials in different environmental and commercial contexts.

Acknowledgments

The authors would like to express their gratitude to the Directorate General of Research and Development (Dirjen Risbang), Ministry of Education, Culture, Research, and Technology (Kemdikbudristek), and LPDP for supporting this research through the Berdikari Grant program under contract number 3228/D6/DV.03.00/2024. Special thanks also to the Politeknik Negeri Media Kreatif for providing facilities and academic support throughout this research.

Author Contributions

Conceptualization, S.A. and H.D.R.; methodology, S.A.; software, H.D.R.; validation, S.A., H.D.R., and N.A.; formal analysis, S.A.; investigation, S.A.; resources, H.D.R.; data curation, A.J.; writing—original draft preparation, S.A.; writing—review and editing, H.D.R.; visualization, A.J.; supervision, H.D.R.; project administration, S.A.; funding

acquisition, H.D.R. All authors have read and agreed to the published version of the manuscript.

Funding
This research was funded by the Directorate General of Research and Development (Dirjen Risbang), Ministry of Education, Culture, Research, and Technology (Kemdikbudristek) and LPDP, grant number 3228/D6/DV.03.00/2024. The APC was funded by the same grant.

Conflicts of Interest
The authors declare no conflict of interest. The funders had no role in the design of the study; in the collection, analyses, or interpretation of data; in the writing of the manuscript; or in the decision to publish the results.

References

Adhikari, J., Bhattarai, A., & Chaudhary, N. K. (2023). Data analysis for SEM-EDX, thermokinetics, surfactant, and corrosion inhibition activity of Co(II) and Zn(II) complexes of pyrrole-based surfactant ligand. *Data in Brief*, *48*, 109124. https://doi.org/10.1016/j.dib.2023.109124

Afdal S, M., Aimon, H., & Satrianto, A. (2019). Analisis Estimasi Produksi Kelapa di Kabupaten Padang Pariaman. *Ecosains: Jurnal Ilmiah Ekonomi Dan Pembangunan*, *8*(2), 167. https://doi.org/10.24036/ecosains.11524157.00

Agarwal, U. P., Ralph, S. A., Baez, C., Reiner, R. S., & Verrill, S. P. (2017). Effect of sample moisture content on XRD-estimated cellulose crystallinity index and crystallite size Effect of sample moisture content on XRD-estimated cellulose crystallinity index and crystallite size. *Cellulose*, *24*(5), 1971–1984. https://doi.org/10.1007/s10570-017-1259-0

Amarakoon, A. M. S. H., & Navaratne, S. (2017). Evaluation of the Effectiveness of Silica Gel Desiccant in Improving the Keeping Quality of Rice Crackers. *International Journal of Science and Research (IJSR)*, *6*(1), 2163–2168. https://doi.org/10.21275/art2017538

Ardiani, S., Rahmayanti, H. D., Akmalia, N., Mulyana, R., & Ikhwannanda, D. (2023). Pendampingan UMKM dan Transfer Teknologi "Nata Gel" di Kelompok Saung Taleus. *Jurnal Pengabdian Masyarakat Progresif Humanis Brainstorming*, *6*(4), 1077–1083. https://doi.org/10.30591/japhb.v6i4.5962

Cheng, J., Gao, R., Zhu, Y., & Lin, Q. (2024). Applications of biodegradable materials in food packaging: A review. *Alexandria Engineering Journal*, *91*(October 2023), 70–83. https://doi.org/10.1016/j.aej.2024.01.080

Clasen, C., Sultanova, B., Wilhelms, T., Heisig, P., & Kulicke, W. (2006). Effects of Different Drying Processes on the Material Properties of Bacterial Cellulose Membranes. *Macromolecule*, *244*(1), 48–58. https://doi.org/10.1002/masy.200651204

Darmawan, R., Susanti, A. A., Kencanaputra, R., & Zikria, R. (2023). *Buku Outlook Komoditas Perkebunan Kelapa*. Pusat Data dan Sistem Informasi Pertanian Sekretariat Jenderal - Kementerian Pertanian.

Fuller, M. E., Andaya, C., & McClay, K. (2018). Evaluation of ATR-FTIR for analysis of bacterial cellulose impurities. *Journal of Microbiological Methods*, *144*(September), 145–151. https://doi.org/10.1016/j.mimet.2017.10.017

Gayathry, G. (2015). Production of Nata de Coco - a Natural Dietary Fibre Product from Mature Coconut Water using Gluconacetobacter xylinum (sju-1) . *International Journal of Food and Fermentation Technology*, *5*(2), 231. https://doi.org/10.5958/2277-9396.2016.00006.4

Guzman-Puyol, S., Benítez, J. J., & Heredia-Guerrero, J. A. (2022). Transparency of polymeric food packaging materials. *Food Research International*, *161*(July). https://doi.org/10.1016/j.foodres.2022.111792

Hamad, A. M. A., Ates, S., & Durmaz, E. (2016). Evaluation of the Possilities for Cellulose Derivatives in Food Products. *Journal of Forestry Faculty*, *16*(2), 383–400. https://doi.org/10.17475/KASTORMAN.289749

Krissanjaya, R. (2024). Karakterisasi Nata De Pina Dari Kulit Nanas PKL dan Madu Kelud sebagai Membran Imobilisator Benedict pada Sensor Optode Pendeteksi Glukosa dalam Darah dan Urin. *Java Health Journal*, *2*(11). https://doi.org/10.1210/jhj.v11i2.701

Latif, A., Ardiani, S., Rahmayanti, H. D., & Situngkir, Y. Y. (2023). Does watermelon rind waste (Citratus Lannatus) have the potential to be an environmentally friendly paper towel ? *AIP Publishing The 10th International Basic Science International Conference (BASIC) 2022*, 1–7. https://doi.org/10.1063/5.0166547

Maulani, T. R. (2018). Karakteristik Sifat Fisikokimia Nata De Taro Talas Beneng Dengan Perbedaan Konsentrasi Acetobacter Xylinum Dan Sumber Karbon. *Jurnal Teknologi Industri Pertanian*, *28*(3), 295–300. https://doi.org/10.24961/j.tek.ind.pert.2018.28.3.296

Maulani, T. R., Hakiki, D. N., & Nursuciyoni, N. (2018). Karakteristik Sifat Fisikokimia Nata De Taro Talas Beneng Dengan Perbedaan Konsentrasi Acetobacter Xylinum Dan Sumber Karbon. *Jurnal Teknologi Industri Pertanian*, *28*(3), 295–300. https://doi.org/10.24961/j.tek.ind.pert.2018.28.3.

296

Mustain, Chodijah, S., Ningsih, A. S., Yudhatama, J., Pramesti, B. A., & Maisela, M. (2022). Pengaruh Konsentrasi Bakteri, Ph, dan Waktu Fermentasi terhadap Produk Nata De Tomato dengan Starter Acetobacter Xylium Teknik Kimia Politeknik Negeri Sriwijaya Comperative Effect of Bacteria Consentration , Time , And Ph on Nata De Tomato Products Usin. *Jurnal Pendidikan Dan Teknologi Indonesia (JPTI)*, *2*(3), 121–125. https://doi.org/10.52436/1.jpti.142

Novia, S., Putri, Y., Syaharani, W. F., Virgiani, C., Utami, B., Safitri, D. R., Arum, Z. N., Prihastari, Z. S., & Sari, A. R. (2021). Pengaruh Mikroorganisme, Bahan Baku, Dan Waktu Inkubasi Pada Karakter Nata : Review The Effect Of Microorganism , Raw Materials, And Incubation Time On The Characteristic Of Nata : A Review Pendahuluan Indonesia merupakan salah satu negara yang memiliki. *Jurnal Teknologi Hasil Pertanian*, *14*(1), 62–74. https://doi.org/10.20961/jthp.v14i1.47654

Nur, S., Said, N., Asyiqin, Z., Syafiq, A., Mohd, F., Ariffin, H., Soplah, S., & Abdullah, S. (2023). The production and characterization of bacterial cellulose pellicles obtained from oil palm frond juice and their conversion to nanofibrillated cellulose. *Carbohydrate Polymer Technologies and Applications*, *5*(May), 100327. https://doi.org/10.1016/j.carpta.2023.100327

Rahmayanti, H. D. (2021). Pendampingan Foto Produk Umkm Komunitas Saung Taleus Di Kota Bogor Menggunakan Ponsel Cerdas. *Jurnal Pekamas*, *1*(2), 79–83. https://doi.org/10.46961/pkm.v1i2.465

Rahmayanti, H. D., Amalia, N., Dewi, Y. C., Sustini, E., & Abdullah, M. (2018). Development of Nata de Coco-based transparent air masks. *Materials Research Express*, *5*(5). https://doi.org/10.1088/2053-1591/aac406

Rahmayanti, H. D., Amalia, N., Yuliza, E., Sustini, E., & Abdullah, M. (2019). Dried nata de coco for extend the shelf life of fruits. *IOP Conference Series: Materials Science and Engineering*, *622*(1), 012010. https://doi.org/10.1088/1757-899X/622/1/012010

Rahmayanti, H. D., Ardiani, S., Akmalia, N., Kartika, T. R., & Suryani, M. (2022). Karakterisasi Sifat Penyerapan Nata de Coco Kering Terpadatkan Terhadap Bolu. *Jurnal Fisika*, *12*(1), 37–41. https://doi.org/10.15294/jf.v12i1.33429

Rahmayanti, H. D., Yuliza, E., Amalia, N., & Abdullah, M. (2024). Dried Nata de Coco with Water Absorptivity Competing Silica Gel. *Indonesian Physical Review*, *7*(2), 250–258. https://doi.org/10.29303/ipr.v7i3.383

Salelatu, J. L., Rumahlatu, D., Program, A., Pendidikan, S., Program, D., & Pendidikan, S. (2016). Pengaruh Lama Fermentasi Terhadap Cita Rasa Nata de Salacca. *Biopendix*, *3*(1), 46–52. https://doi.org/10.30598/biopendixvol3issue1page46-52

Shaikh, S., Yaqoob, M., & Aggarwal, P. (2021). An overview of biodegradable packaging in food industry. *Current Research in Food Science*, *4*, 503–520. https://doi.org/10.1016/j.crfs.2021.07.005

Suhaendah, E., Fauziyah, E., P, L. A. G., & Sudomo, A. (2021). Pertumbuhan Talas Beneng (Xanthosoma undipes K. Koch) pada Pola Agroforestri. *Jurnal Agroforestri Indonesia*, *4*(1), 61–68. https://doi.org/10.37149/jia.v9i2.1150

Sutanto, A. (2012). Pineapple Liquid Waste As Nata De Pina Raw Material. *MAKARA of Technology Series*, *16*(1). https://doi.org/10.7454/mst.v16i1.1286

Syaifudin, A., Kamulyan, B., Mardiana, D., Kimia, J., Matematika, F., Alam, P., & Brawijaya, U. (2015). Pemanfaatan Nata De Coco Termodifikasi Asam Sitrat Sebagai Bahan Baku Membran. *Kimia Student Journal*, *1*(1), 723–729. Retrieved from https://media.neliti.com/media/publications/249834-none-289ec306.pdf

Yano, S., Maeda, H., & Nakajima, M. (2007). *Preparation and mechanical properties of bacterial cellulose nanocomposites loaded with silica nanoparticles*. *135*, 1–4. https://doi.org/10.1007/s10570-007-9152-x

Yasa, I. W. S., Eko Basuki, S. S., & Handito, D. (2020). Sifat Fisik Dan Mekanis Lembaran Kering Selulosa Bakteri Berbahan Dasar Limbah Hasil Pertanian. *JRPB*, *8*(1), 89–99. https://doi.org/10.29303/jrpb.v8i1.170